Cell Reports, Volume *30*

Supplemental Information

Cancer Cells Resist Mechanical Destruction in Circulation via RhoA/Actomyosin-Dependent Mechano-Adaptation

Devon L. Moose, Benjamin L. Krog, Tae-Hyung Kim, Lei Zhao, Sophia Williams-Perez, Gretchen Burke, Lillian Rhodes, Marion Vanneste, Patrick Breheny, Mohammed Milhem, Christopher S. Stipp, Amy C. Rowat, and Michael D. Henry

Figure S1

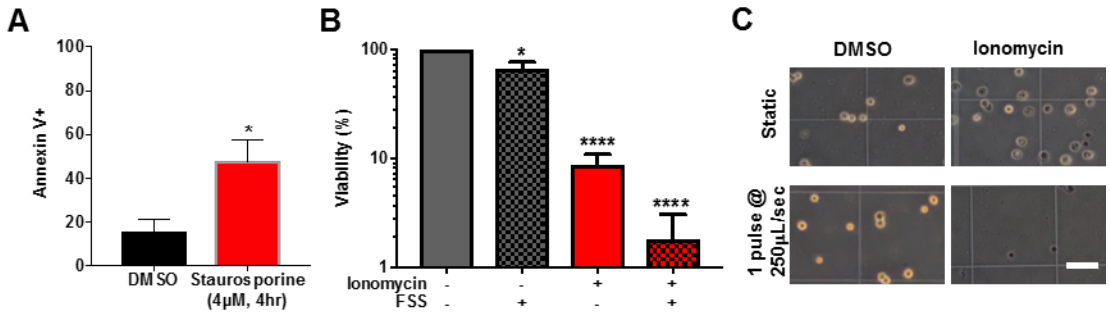

Figure S1 related Figure 1: Dead cancer cells are rapidly fragmented by FSS. A) Apoptosis in PC-3 cells treated with staurosporine (4μM, 4hr), as assessed by Annenxin V staining (*p<0.05, n=4; t-test). B) Effects of ionomycin treatment (10 μM, 30 min) on susceptibility of PC-3 cells to 1 pulse of FSS at 250 μL/s. DMSO is vehicle control for ionomycin treatment. Ionomycin treatment significantly reduced viability (****p<0.0001, n=3; 1-way ANOVA with Bonferroni) and sensitized cells to FSS (****p<0.0001, n=3; 1-way ANOVA with Bonferroni) while the reduction in viability due to shear stress alone was not as great (*p<0.05, 1-way ANOVA with Bonferroni). C) Phase-contrast images of cells before and after ionomycin treatment and/or FSS exposure. Bar, 100μm. Data is presented as mean with SEM error bars.

Figure S2

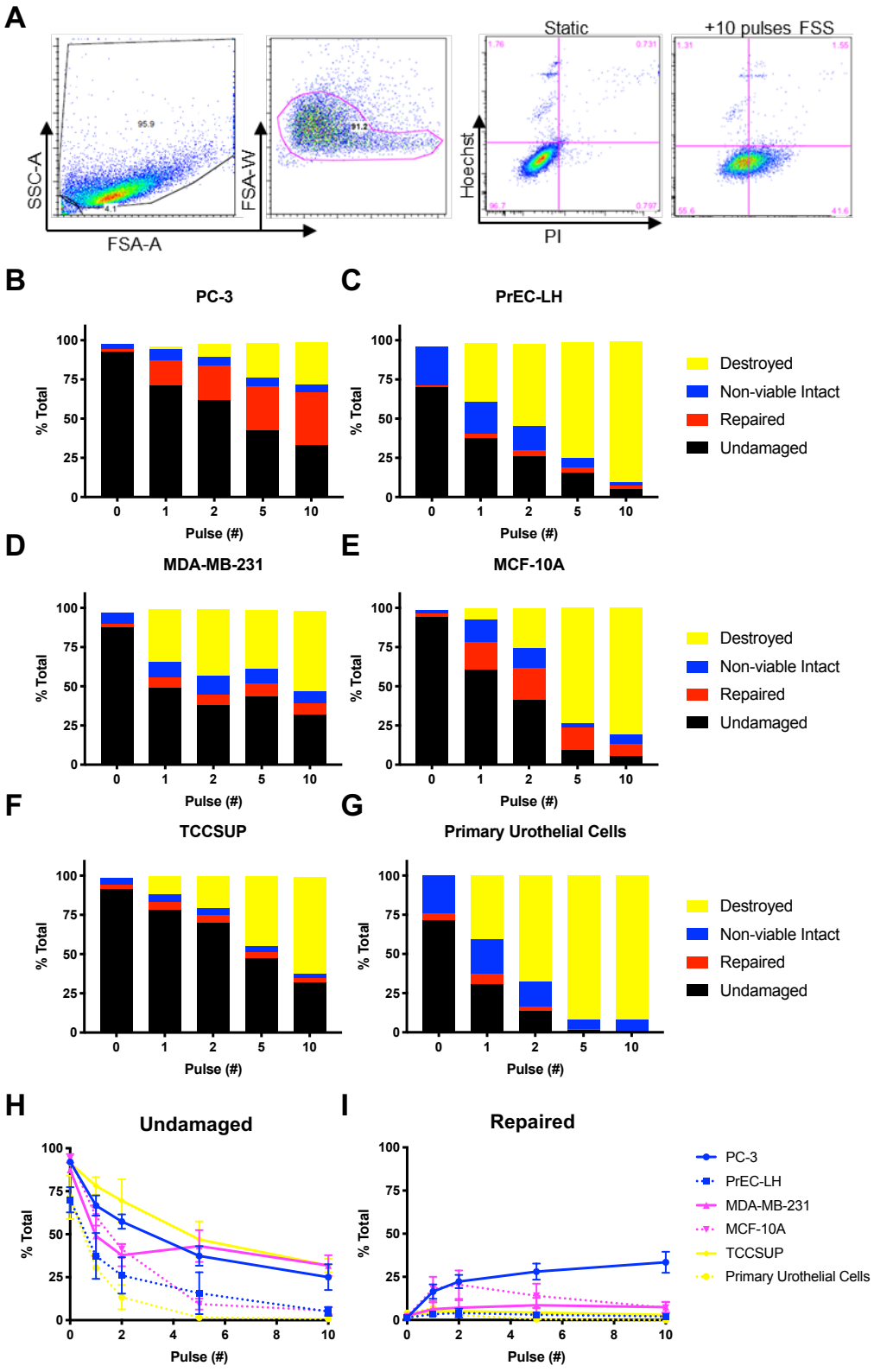
A
SSC-A
FSA-A
FSA-W
Static
+10 pulses FSS
Hoechst
PI
B
PC-3
C
PrEC-LH
D
MDA-MB-231
E
MCF-10A
F
TCCSUP
G
Primary Urothelial Cells
% Total
Pulse (#)
Destroyed
Non-viable Intact
Repaired
Undamaged
H
Undamaged
I
Repaired
PC-3
PrEC-LH
MDA-MB-231
MCF-10A
TCCSUP
Primary Urothelial Cells

Figure S2 related to Figure 2: Transformed cells have a higher resistance to FSS induced plasma membrane damage than their non-transformed counterparts. A) Representative gating profile with PI and Hoechst stain for static and sheared PC-3 cells (10 pulses). B-G) Histograms showing population means over the course of exposure for undamaged, repaired, nonviable intact, and destroyed fractions for paired transformed (PC-3, MDA-MB-231, TCCSUP) and non-transformed (PrEC-LH, MCF10A, and primary urothelial cells) cells from prostate (B&C), breast (D&E), and bladder (F&G) over multiple pulses (0, 1, 2, 5, & 10). H) Undamaged fraction for indicated cell lines over the course of FSS exposure. Solid lines indicate transformed cells and dashed lines indicate non-transformed lines. The capacity to resist damage correlates with transformation status ($p<0.0001$; repeated measures three-way ANOVA). I) Repaired fraction for the 3 paired cell lines over the course of FSS exposure for the same experiment shown in H. Membrane repair does not correlate with transformation status ($p>0.05$; repeated measures three-way ANOVA). Data in (B-G) are presented as mean and data in (H) and (I) are presented as mean with SEM error bars.

Figure S3

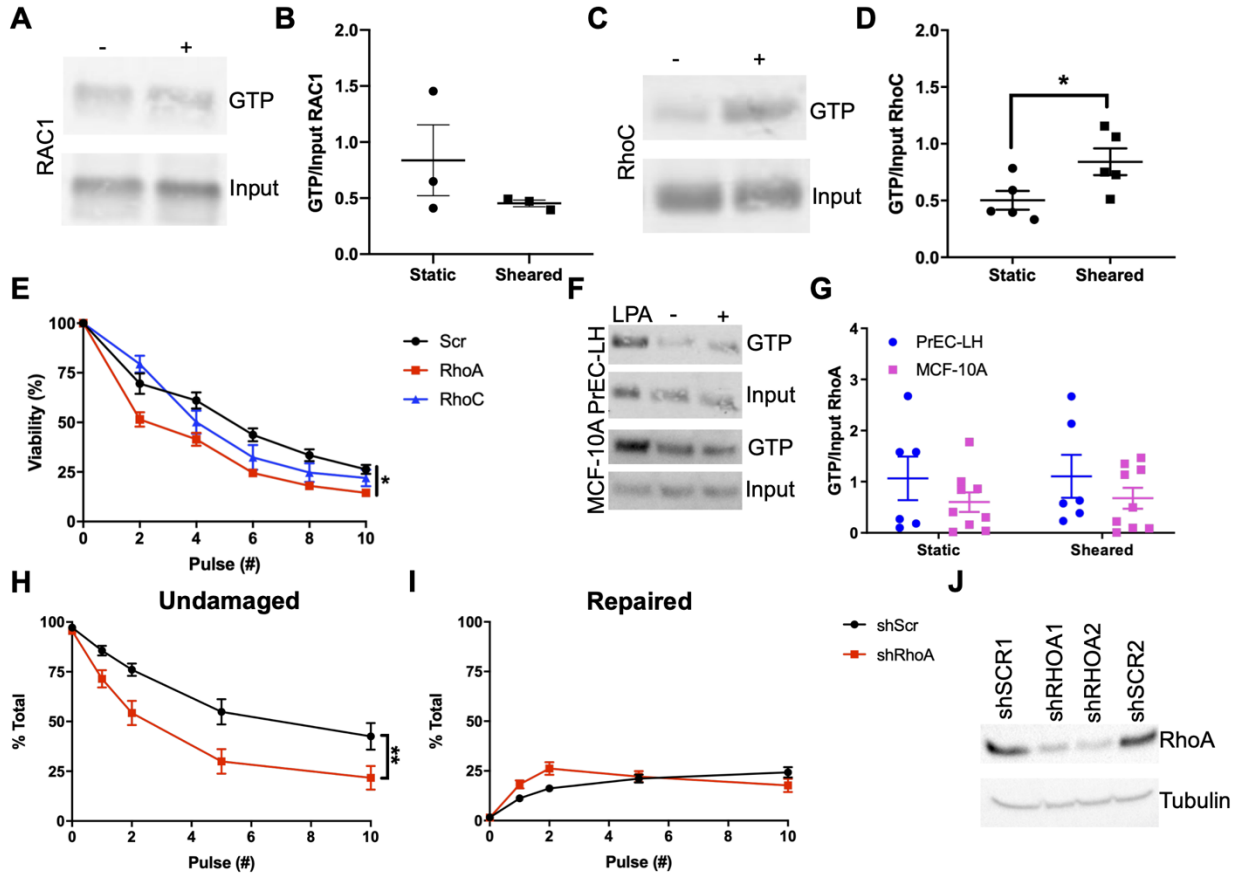

Figure S3 related to Figure 3: Exposure to FSS activates Rho and not RAC family GTPase. A) RAC1 pulldown blot for static (-) and sheared (+) cells and B) analysis of RAC1 activity assay indicating that GTP-RAC1 levels do not change in response to FSS ($p>0.05$, n=3, T-test). C) RhoC pulldown blot for static (-) and sheared (+) cells and D) analysis RhoC activity assay data demonstrating an increase in GTP bound RhoC after FSS exposure ($p<0.05$, n=5, T-test). E) Data of viability after exposure to FSS for GS689.Li cells expressing shRNA against RhoA (n=6), RhoC(n=6), or non-targeting control (SCR) (n=12). RhoA knockdown cells have significantly reduced viability from pulse number 2 to 10 in comparison to SCR cells ($p<0.05$, t-test with Bonferroni correction), while RhoC does not cause a significant change in viability ($p>0.05$, t-test with Bonferroni correction). F) RhoA pulldown for MCF-10A and PrEC-LH cells under static (-) and sheared (+) conditions and G) quantification of pulldowns, with no significant alterations of RhoA activity after FSS exposure. H) Inhibition of RhoA significantly reduces undamaged fraction compared to SCR control cells (**$p<0.01$; 2-way ANOVA, n=9/group), I) while the effects of RhoA knockdown on membrane repair is not statistically significant ($p>0.05$; 2-way ANOVA, n=9/group). J) Western blot of PC-3 cells with control shRNA and shRNA against RHOA, showing RhoA knockdown. Data in (B), (D), (E), (G-I) are presented as mean with SEM error bars.

Figure S4

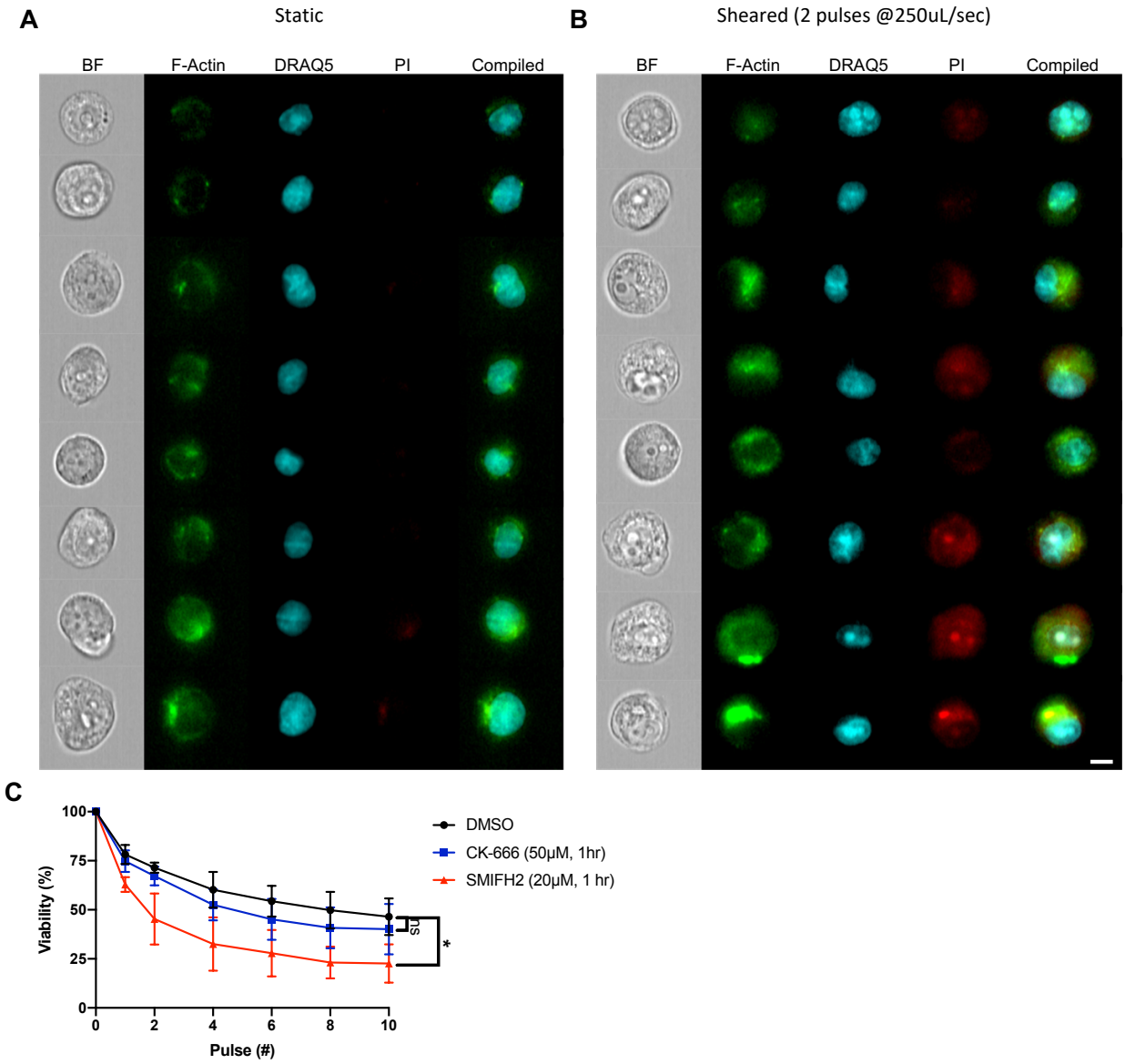

Figure S4 related to Figure 3: PC-3 cells increase cortical F-actin in response to FSS. A-B) Imagestream images of PC-3 cells stained for F-actin that were under static (A) or sheared (B) conditions. C) Viability of PC-3 cells after FSS exposure when pre-treated with a control (DMSO), Arp2/3 (CK-666) inhibitor, and formin inhibitor (SMIFH2) (* p>0.05; 2-way ANOVA, n=3/treatment). Data in (C) are presented as mean with SEM error bars.

Figure S5

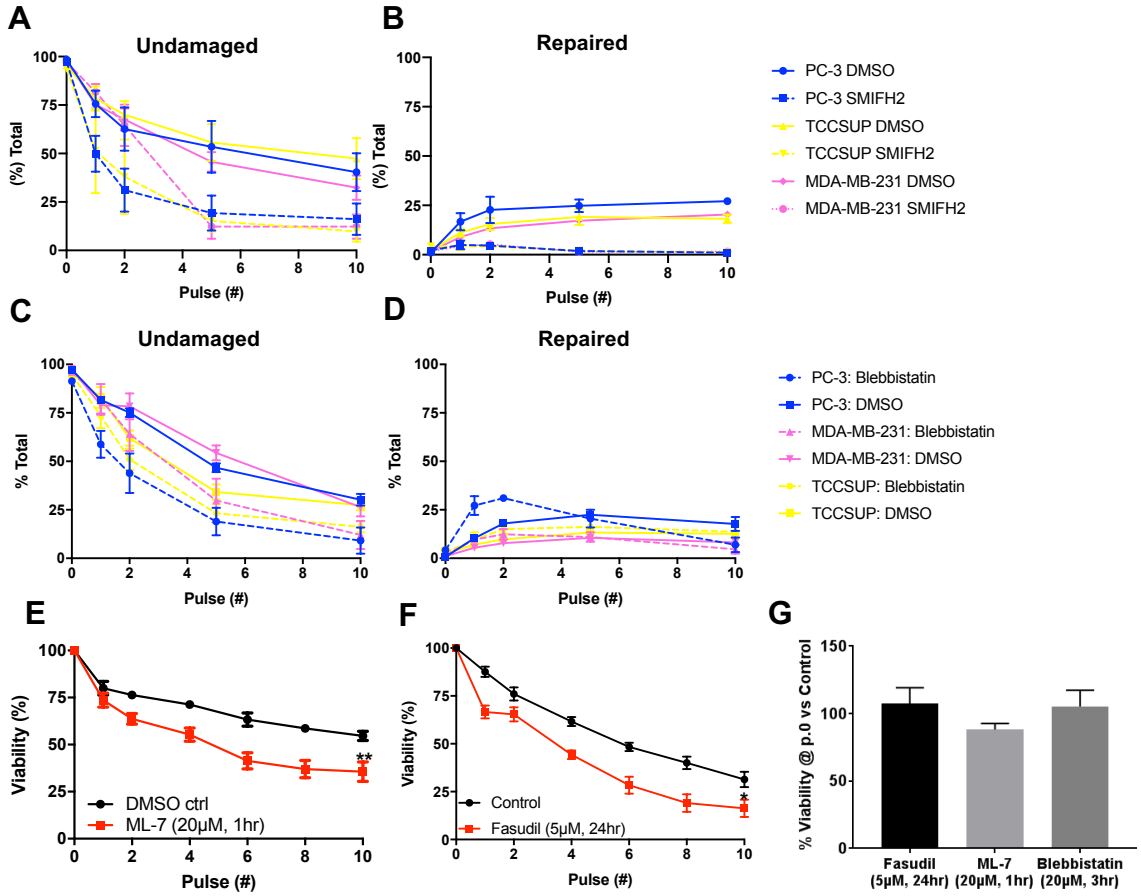

Figure S5 related to Figure 3: Cancer cells depend on acto-myosin activity to resist plasma membrane damage. A) Fraction of PC-3, TCCSUP, and MDA-MB-231 cells that do not have detectable membrane damage after FSS exposure, with DMSO (solid line) or SMIFH2 (20μM, 1hr)(dashed line) treatment. A 3-way ANOVA has the treatment of SMIFH2 significantly contributing to reduction in the undamaged fraction ($p<0.0001$, n=3/cell line). B) Fraction of cells from the experiment in (A) that have undergone detectable membrane repair, which was signifantly reduced upon SMIFH2 treatment ($p<0.0001$, 3-way ANOVA, n=3/cell line). C) A 3 way ANOVA of the undamaged data demonstrated that blebbistatin treatment accounted for a significant portion of the variability ($p<0.01$, n=3/cell line) and that the response to blebbistatin treatment did not depend on the cell line ($p>0.05$). Additionally, blebbistatin treatment influenced how the cells responded to each pulse of FSS ($p<0.001$). D) 3-way ANOVA of the membrane repair data demonstrates that membrane repair is different among cell lines ($p<0.0001$) and it is impacted by blebbistatin treatment ($p<0.05$). E) ML-7, myosin light-chain kinase inhibitor, (20μM, 1hr) sensitizes PC-3 cells to FSS (**$p<0.01$ 2-way ANOVA, n=3). F) Pre-treatment with fasudil, a ROCK inhibitor, (5μM, 24 hr) sensitizes PC-3 cells to FSS (*$p<0.05$, 2-way ANOVA, n=8). G) None of these agents significantly reduced the viability of cells prior to FSS exposure. Data in (A-G) are presented as mean with SEM error bars.

Figure S6

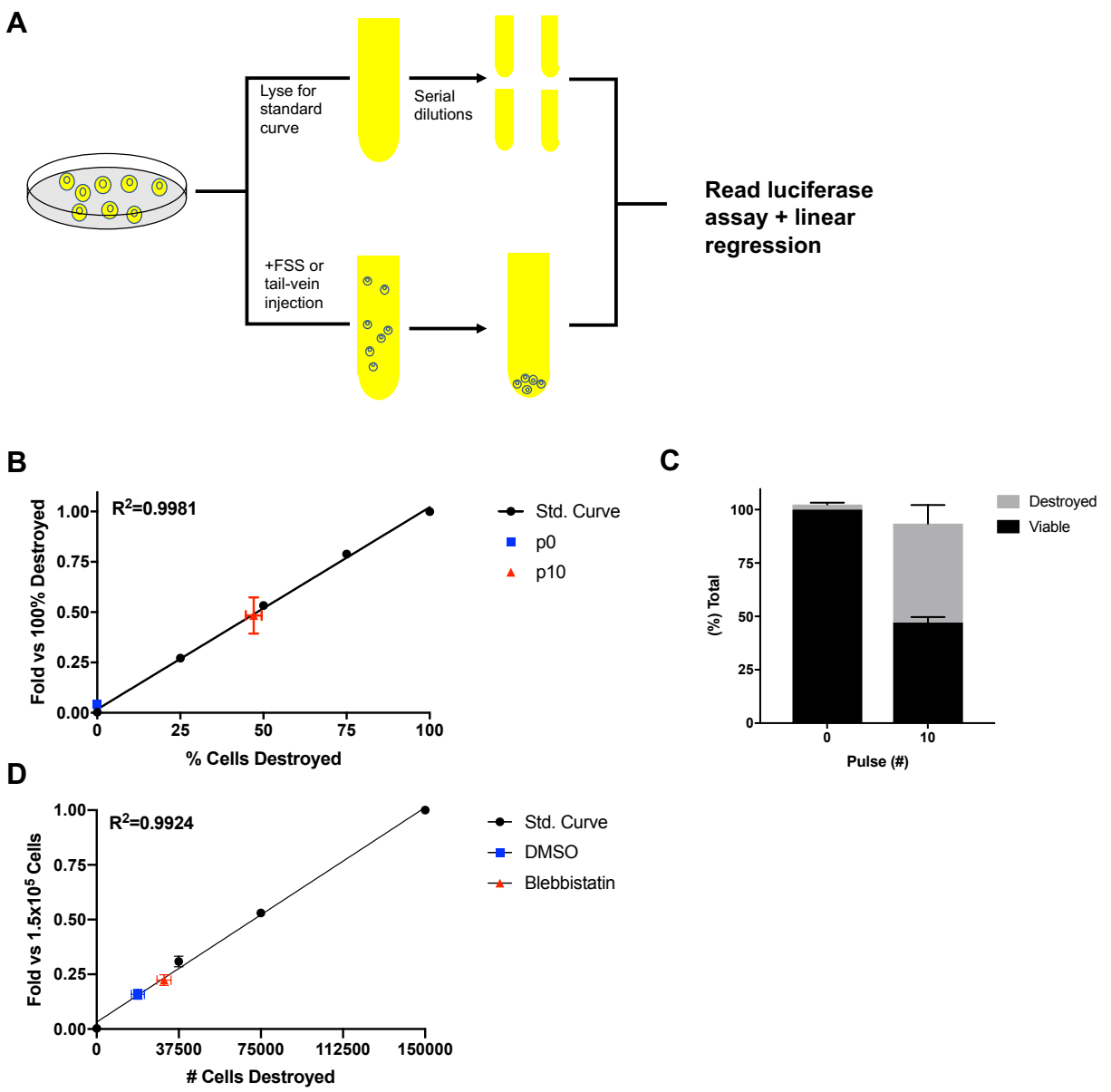

Figure S6 related to Figure 4: Validation of assay for measuring cell destruction based on levels of cell-free luciferase. A) Schematic of experimental workflow. B) Graph of the compiled data from the standard curves from lysed cells and supernatant from sheared cells used for validating the method with the in vitro FSS assay. C) Bar graph showing that the cell-free luciferase assay in (B) accurately accounts for the loss of viability from sheared cells ($p>0.05$; t-test). D) Standard curve and luciferase signal from the plasma of mice injected with cells compiled from 4 independent experiments, 2 with DMSO-treated cells expressing luciferase (n=7 mice) and 2 with blebbistatin-treated cells expressing luciferase (n=6 mice). Data in (B-G) are presented as mean with SEM error bars.

Figure S7

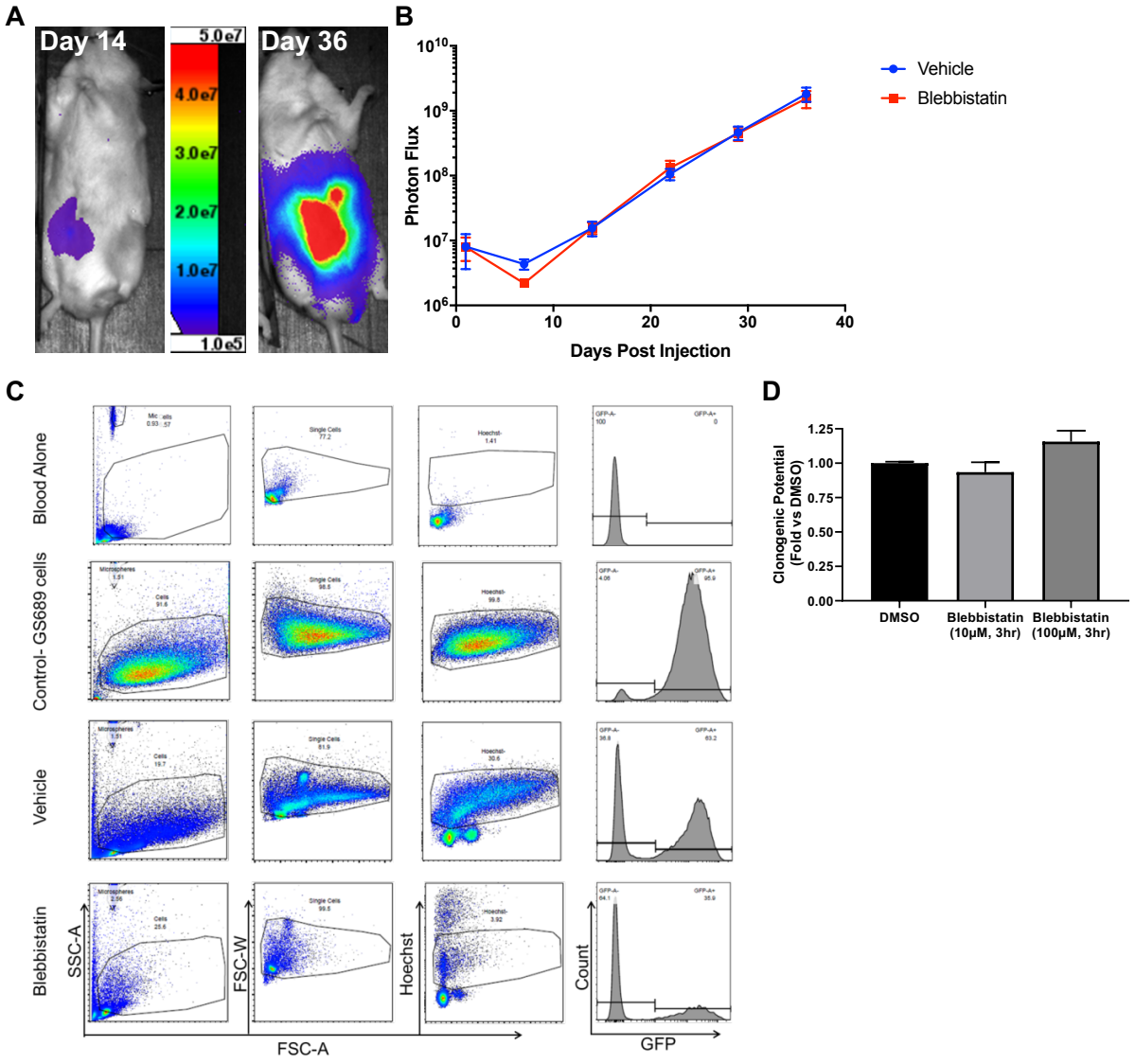

Figure S7 related to Figure 6: Blebbistatin reduces steady-state CTC number. A) Example BLI images and B) analysis of mouse tumor burden segregated by end group assignment, showing that tumor burden and growth did not different significantly between the vehicle and blebbistatin-treated groups ($p>0.05$; 2-way ANOVA). C) Flow analysis of blood alone, parental cells, blood from a vehicle treated mouse, and blood from a blebbistatin-treated mouse used to establish gating parameters. D) Clonogenic assay of GS689 cells treated with DMSO, 100μM (estimated maximum concentration) and 10μM of blebbistatin for 3 hours, demonstrating that the dose was not directly cytotoxic to cancer cells. Data in (B) and (D) are presented as mean with SEM error bars.

Figure S8

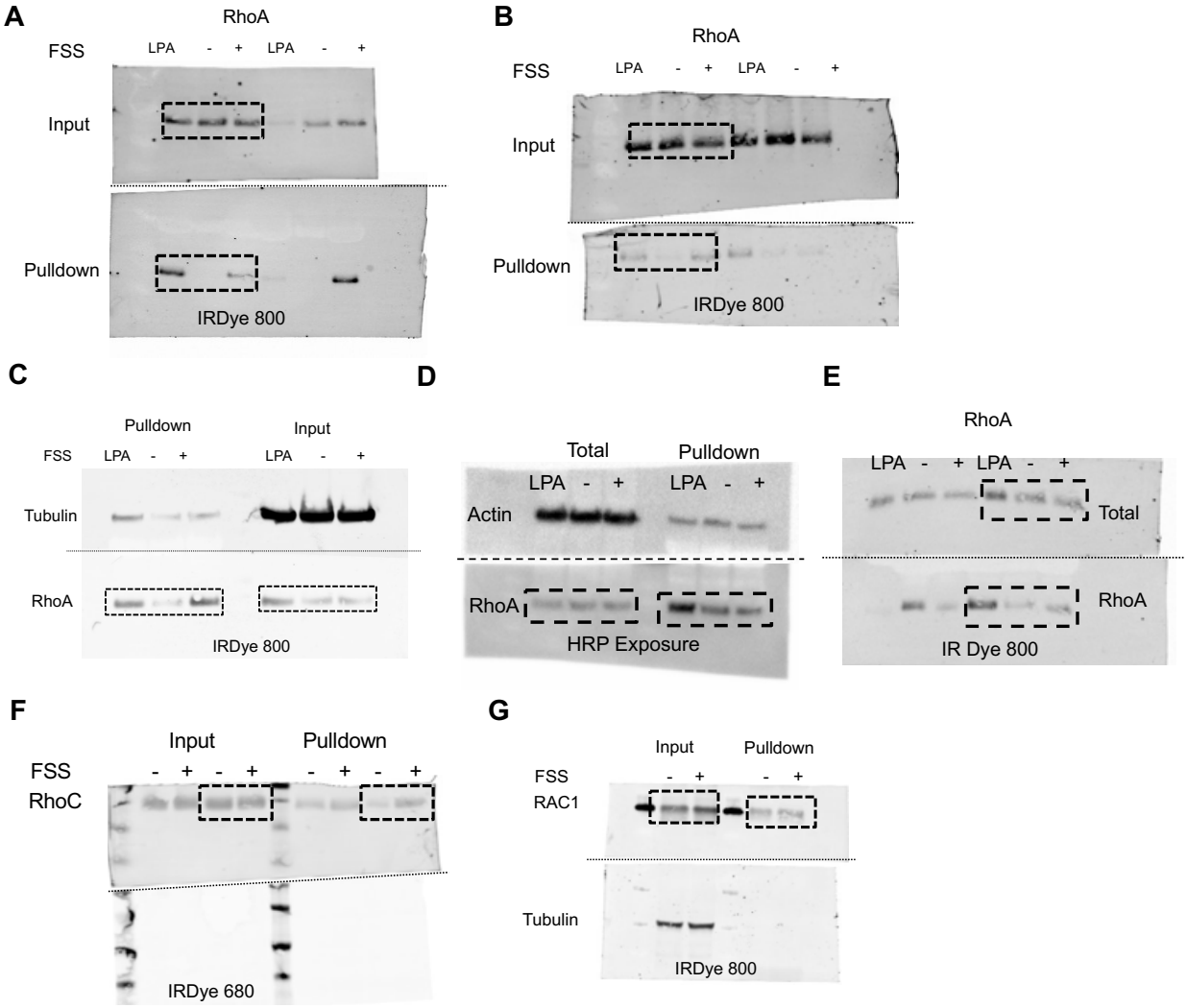

Figure S8 related to Figure 3; S3: Western blot scans of Rho Family activity assays. Dotted line indicate where blot was cut to incubate with additional primary, dashed box indicate what is presented. Western for RhoA pulldown from A) PC-3 cells B) MDA-MB-231 cells, C) TCCSUP, D) MCF-10A, and E) PrEC-LH cells. Western of PC-3 cells that have been exposed to FSS for F) RhoC pulldown and G) RAC1 pulldown.

Figure S9

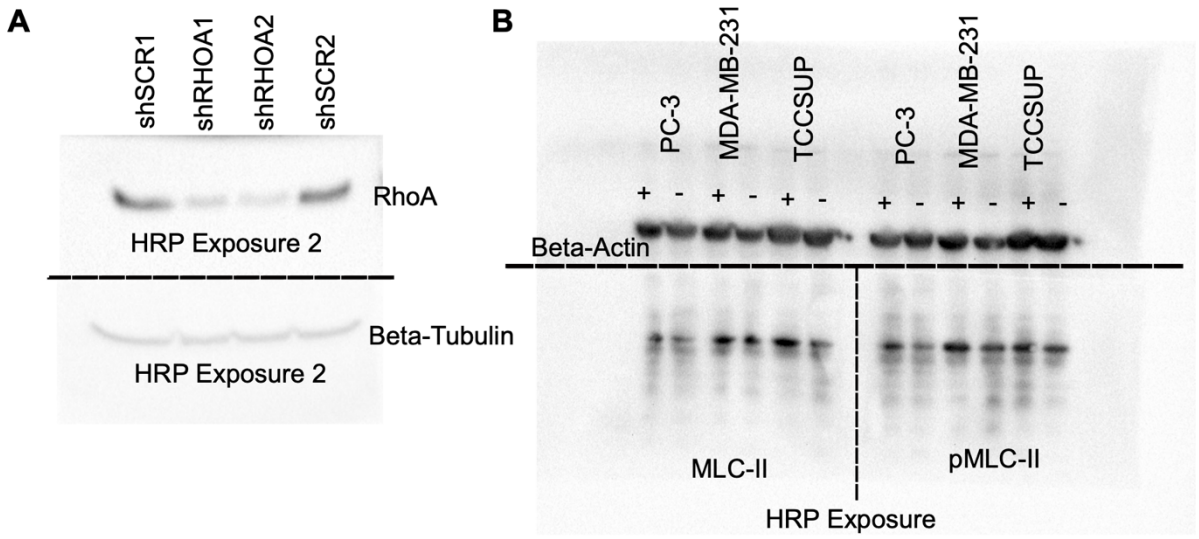

Figure S9 related to Figures 3, S3: Western blot scans presented throughout the paper. A) Western of RhoA knockdown in PC-3 cells. B) Western of PC-3, MDA-MB-231, and TCCSUP cells that have been held under static conditions (-) or exposed to two pulses of FSS (+).

Sample ID	DMSO	Blebbistatin	Microsphere Count	% Microsphere Inj.	% Inj. Cells Destroyed
Control 1	677	658	46	N/A	N/A
Mouse 1	2993	2781	433	0.87%	0.8%
Mouse 2	3991	3359	518	1.04%	2.6%
Mouse 3	4577	3952	487	0.97%	4.2%
Mouse 4	2926	2461	328	0.66%	4.1%
Control 2	669	1103	61	N/A	N/A
Mouse 6	2311	2813	318	0.64%	3.2%
Mouse 7	3027	3743	427	0.85%	6.1%
Mouse 8	2473	3582	387	0.77%	5.3%

Table 1 related to Figure 4: **Fewer blebbistatin-treated cells lodge in the lung microvasculature.** Data from 2 independent animal experiments with colors corresponding to the dye used (Blue for Cell-Tracker Red and Green for Cell-Tracker Green), showing the count of nucleated cells as well as microspheres from whole lung section images. % injected cells destroyed column is based on cell-free plasma luciferase data and is colored to match the detection for which treatment group was measured.